3D Structural Analysis of AGL Proteins

AGL15: Comparative 3D Structural Analysis

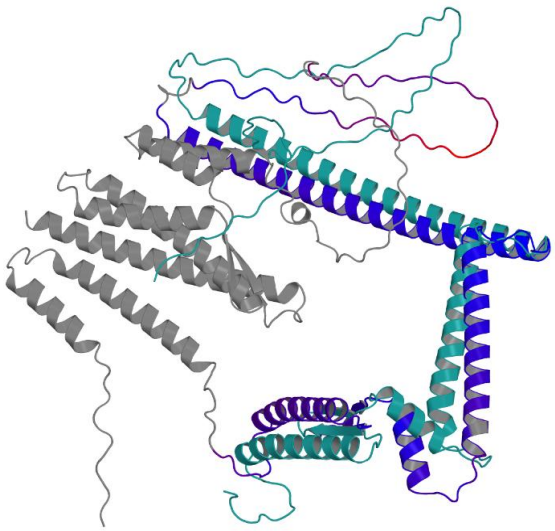


Figure S1: Three-dimensional structural analysis of AGL15. Three-dimensional models of AGL15 (15357_ath_agl15) and A0A7J0FVE2 were generated using AlphaFold. The A0A7J0FVE2 structure is shown in green, while the 15357_ath_agl15 structure is colored according to the RMSD-based structural comparison. Regions showing good structural agreement are highlighted in blue, structurally divergent regions are shown in red, and regions that could not be aligned are shown in gray. The structural comparison revealed approximately 45% overall structural similarity between AGL80 and A0A7J0FW04. The major structural differences were observed toward the N- and C-terminal regions of the structure, whereas the central regions showed greater structural correspondence.

AGL61: Comparative 3D Structural Analysis

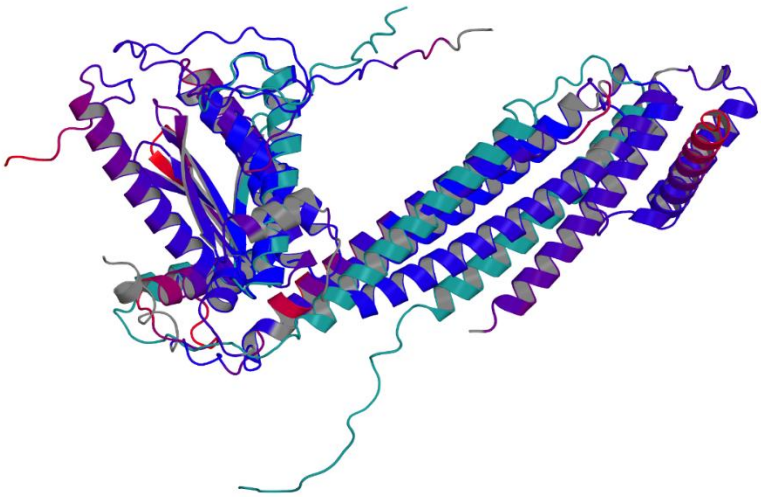


Figure S2: Three-dimensional structural analysis of AGL61. Three-dimensional models of AGL61 (46683_ath_AGL61, 10198_ath_AGL61, 29968_ath_AGL61, and 1393_ath_AGL61) and A0A7J0EUU1 were generated using AlphaFold. The A0A7J0EUU1 structure is shown in green, while the AGL61 structures are colored according to the RMSD-based structural comparison. Regions exhibiting good structural agreement are shown in blue, structurally divergent regions are shown in red, and regions that could not be reliably aligned are shown in gray. Overall, the structural comparison revealed a high degree of structural similarity between the AGL61 models and A0A7J0EUU1. The most pronounced structural differences were observed toward the N- and C-terminal regions, which were removed from the visualization to facilitate comparison of the conserved structural regions. In contrast, the central regions showed greater structural correspondence between the AGL61 models and the reference structure.

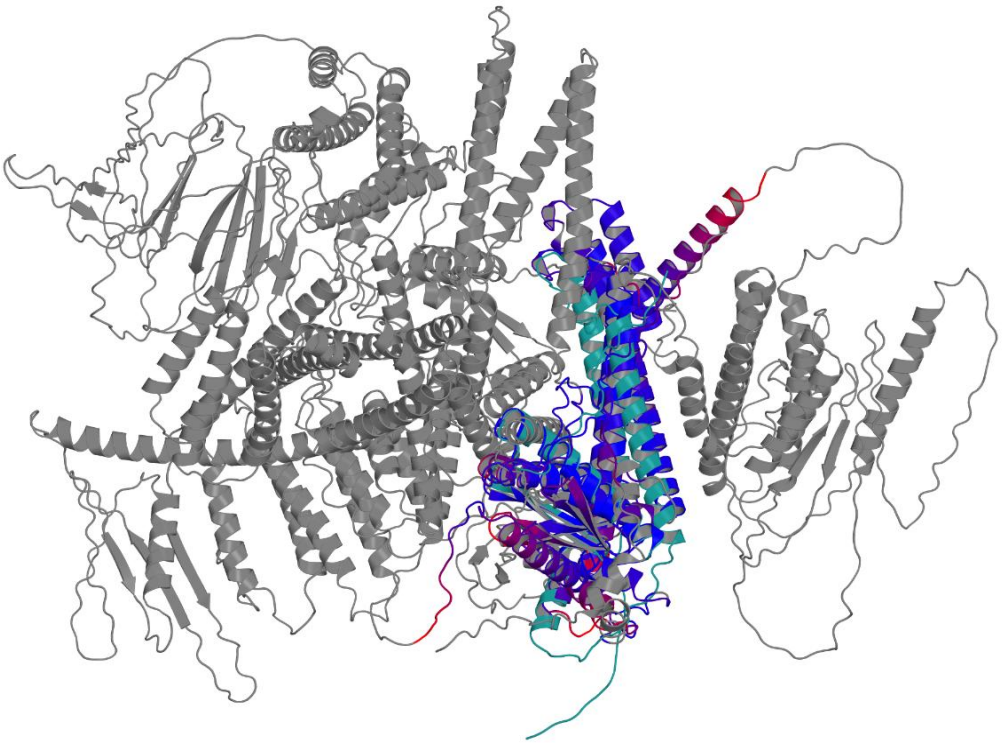


Figure S3: Three-dimensional structural analysis of AGL61. Three-dimensional models of AGL61 (46683_ath_AGL61, 10198_ath_AGL61, 29968_ath_AGL61, and 1393_ath_AGL61) and A0A7J0EUU1 were generated using AlphaFold. The A0A7J0EUU1 structure is shown in green, while the AGL61 structures are colored according to the RMSD-based structural comparison. Regions exhibiting good structural agreement are shown in blue, structurally divergent regions are shown in red, and regions that could not be reliably aligned are shown in gray. Overall, the structural comparison revealed a high degree of structural similarity between the AGL61 models and A0A7J0EUU1, particularly within the central regions of the proteins. The most pronounced structural differences were observed toward the N- and C-terminal regions, where greater structural divergence and regions of poor or unsuccessful alignment were detected. The complete structures, including both terminal regions, are shown to provide a comprehensive representation of the structural similarities and differences between the AGL61 models and the reference structure.

AGL62: Comparative 3D Structural Analysis

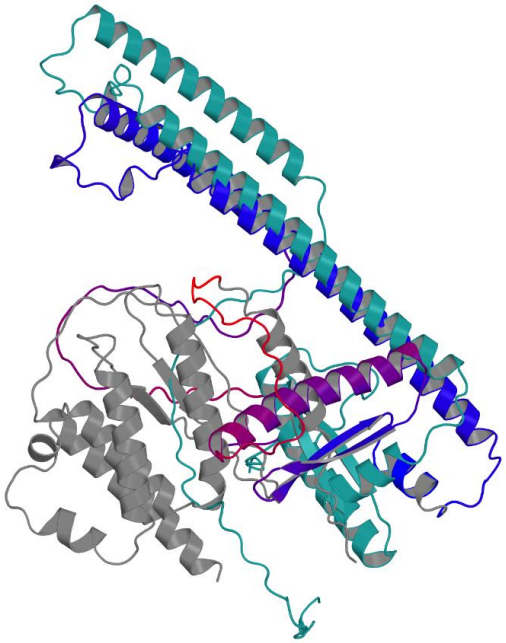


Figure S4: Three-dimensional structural analysis of AGL62. Three-dimensional models of AGL62 (7944_aruf_agl62) and A0A7J0EQ66 were generated using AlphaFold. The A0A7J0EQ66 structure is shown in green, while the 7944_aruf_agl62 structure is colored according to the RMSD-based structural comparison. Regions showing good structural agreement are highlighted in blue, structurally divergent regions are shown in red, and regions that could not be aligned are shown in gray. The structural comparison revealed approximately 40% overall structural similarity between AGL62 and A0A7J0EQ66. The major structural differences were observed toward the N- and C-terminal regions of the proteins, whereas the central regions showed greater structural correspondence.

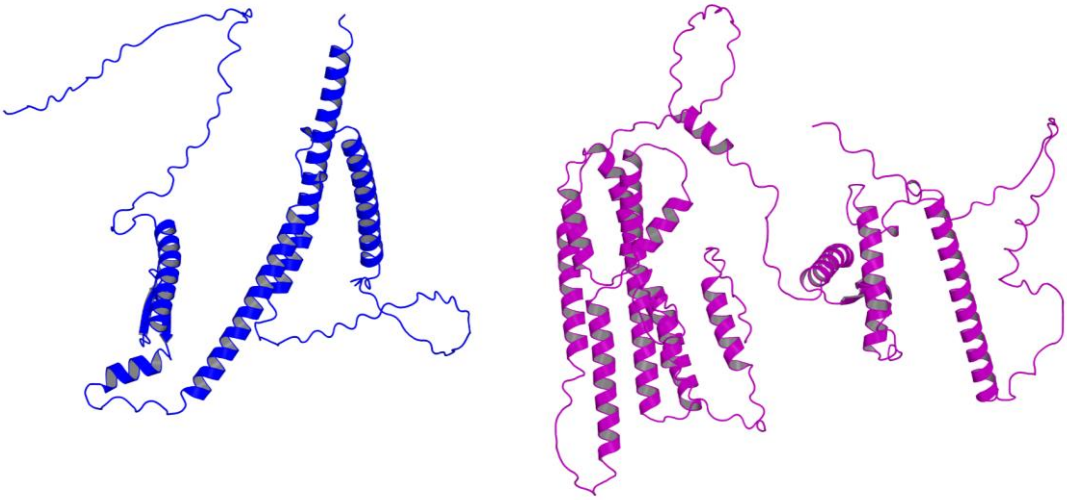


Figure S5: Three-dimensional structural analysis of AGL62. The predicted three-dimensional structures of 68068_ath_AGL62 (left, blue) and 104080_ath_AGL62 (right, purple) are shown. Structural analysis revealed differences between the two predicted models that prevented successful alignment with the reference structure. These structural discrepancies highlight the need for further structural analysis to assess and validate the predicted structures of the annotated AGL62 sequences.

AGL80: Comparative 3D Structural Analysis

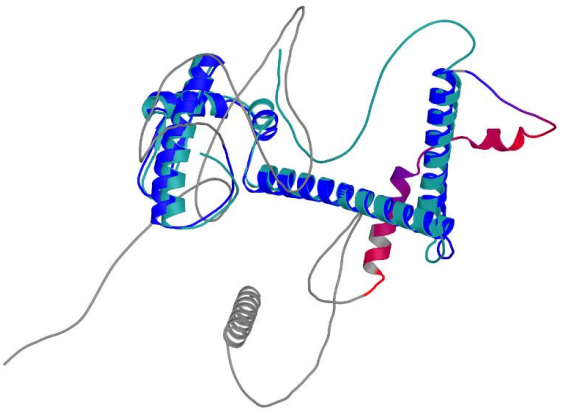


Figure S6: Three-dimensional structural analysis of AGL80. Three-dimensional models of AGL80 (17213_ath_agl80) and A0A7J0FW04 were generated using AlphaFold. The A0A7J0FW04 structure is shown in green, while the 17213_ath_agl80 structure is colored according to the RMSD-based structural comparison. Regions showing good structural agreement are highlighted in blue, structurally divergent regions are shown in red, and regions that could not be aligned are shown in gray. The structural comparison revealed approximately 30% overall structural similarity between AGL80 and A0A7J0FW04. The major structural differences were observed toward the N- and C-terminal regions of the proteins, whereas the central regions showed greater structural correspondence.

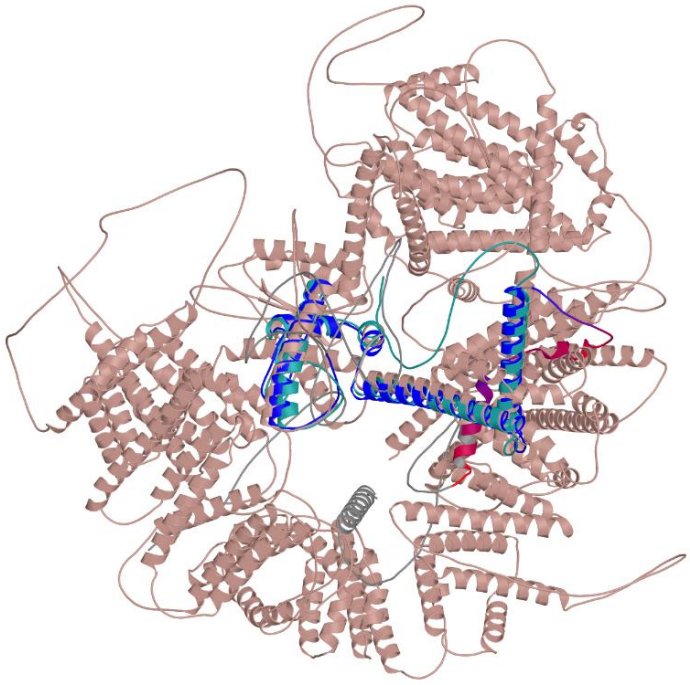


Figure S7: Three-dimensional structural analysis of AGL80. Three-dimensional models of AGL80 (17213_ath_agl80 and 32624_ath_agl80) and A0A7J0FW04 were generated using AlphaFold. The A0A7J0FW04 structure is shown in green, 32624_ath_agl80 in salmon, while 17213_ath_agl80 is colored according to the RMSD-based structural comparison. The 32624_ath_agl80 model showed alignment with A0A7J0FW04 only over a short structural region. This limited structural correspondence may reflect potential issues with the underlying sequence, including possible sequence-quality or annotation errors, or limitations associated with the predicted AlphaFold model. Therefore, the 32624_ath_agl80 sequence and its corresponding structural prediction should be further investigated and experimentally or computationally validated to confirm the predicted protein structure.Consistent with the structural analysis, the phylogenetic analysis places 32624_ath_agl80 on a relatively long branch, indicating a high level of sequence divergence from the other AGL80 sequences included in the analysis. This pronounced divergence further supports the need for additional investigation to determine whether the observed differences reflect genuine evolutionary divergence or may be influenced by sequence quality, annotation, or other model-related factors.